JOURNAL OF SOLID STATE CHEMISTRY **134,** 91–98 (1997)
ARTICLE NO. SC977541

Gallium Phosphate Thin Films: Synthesis and Dielectric Properties

F. Tourtin,* P. Armand,[1,]* A. Ibanez,† and E. Philippot*

*LPMC, UMR 5617 CNRS, UMII, Case 003, Place E. Bataillon, 34095 Montpellier Cedex 05, France
† Laboratoire de cristallographie, CNRS, 25 avenue des Martyrs, BP 166, 38042 Grenoble Cedex 09, France

Received February 18, 1997; in revised form July 8, 1997; accepted July 10, 1997

Deposits of dielectric gallium phosphate thin films on silicon and gallium arsenide semiconductors have been obtained by pyrolysis of an aerosol produced by ultrasonic spraying ("pyrosol" process) and containing the organometallic precursors gallium acetylacetonate and tributyl phosphate. The composition and microstructure of the layers are discussed with respect to the experimental conditions. For this paper, electrical properties were also studied. Using the metal–insulator–semiconductor structure, the behavior of conductivity under direct current, capacitance, and dielectric loss was studied in terms of frequency, temperature, and chemical composition. The sites involved in the conduction process are structural defects directly related to the oxygen excess present in deposits which leads to the formation of *M*–O dangling bonds (*M* = Ga or P).

I. INTRODUCTION

III–V semiconductor compounds are characterized by remarkable intrinsic properties (high electronic mobility). Nevertheless, their use in electronic devices such as metal–insulator–semiconductor field effect transistors (MISFETs) is limited by the difficulty in forming high-quality insulating thin films on their surface. III–V native oxides are generally chemically inhomogeneous and give insulator semiconductor interfaces with poor electrical properties (1). This is unlike the case of silicon, where oxidation at the surface of the material can be controlled precisely so as to produce an insulating layer of amorphous silica with convenient electronic properties. Since it is established that the α form of both $AlPO_4$ (berlinite) and $GaPO_4$ crystals has interesting dielectric and piezoelectric characteristics better than those of the α-quartz (2–5), we are developing a method of depositing these materials as thin films on III–V semiconductors. In previous works, we coated aluminum phosphate thin films on silicon substrates (6–8); now, we are working on the synthesis of gallium phosphate thin films on Si and GaAs substrates. Gallium phosphate, which exhibits good dielectric properties, seems to be a good candidate for passivating III–V semiconductors such as GaAs, by use of a low-temperature deposition method, the "pyrosol" process. This method is based on the thermolysis of an aerosol produced from a solution containing the organometallic precursors. This solution is pulverized on the surface of the liquid with an ultrasonic source. The resultant mist is propelled by a vector gas (air or nitrogen) toward the heated substrate. On contact, the solvent is vaporized and the precursors are cracked, inducing the formation of thin homogeneous layers (9, 10). In this paper, we first report the experimental conditions under which the gallium phosphate layers are obtained. Two parameters are examined: the concentration of the starting solution containing the precursors and the deposit temperature. Their influence on growth rate, chemical composition, morphology, and crystallinity is discussed in Section II, where we show the effect of thermal treatment on the deposits. In Section III, we present the electrical properties of gallium phosphate thin films by studying metal–insulator–semiconductor (MIS) capacitors. We first determine the conductivity from direct measurements and then report the temperature and the frequency dependence of the real part of the dielectric constant as well as the imaginary part (dielectric loss). These studies have been undertaken to gain a better understanding of the nature of the defects and, so, to be able to enhance the dielectric properties of gallium phosphate thin films.

[1] To whom correspondence should be addressed.

II. DEPOSITION AND CHARACTERIZATIONS OF GALLIUM PHOSPHATE LAYERS

1. Experimental Procedure

Gallium phosphate thin films were obtained by the "pyrosol" process (pyrolysis of an aerosol). In this process, low-molar-concentration solutions of various metallic organic compounds are sprayed on a heated substrate. In the vinicity of the substrate surface, pyrolysis occurs and films are deposited. The mechanism, which leads to good films in terms of adherence, crystallinity, and thickness, is a chemical vapor deposition (CVD) process (9, 10).

0022-4596/97 $25.00

In this work, the experimental setup is derived from the pyrosol process (11). The starting solution consists of a mixture of two precursors: tributyl phosphate [TBP, $(C_4H_9)_3PO_4$; for synthesis, 99% min, Merck] at various concentrations (0.025, 0.050, and 0.075 M) and gallium acetylacetonate [GaAA, $Ga(C_5H_7O_2)_3$; synthesized in the laboratory by the action of acetylacetone; for synthesis, 99% min, Merck, on freshly precipated gallium hydroxide (12) (yield > 90%)] at fixed concentration [0.025 M in ethanol (maximum solubility)]. These precursors were chosen from previous works on thin layers deposited by the "pyrosol" process (9, 11, 13), as $AlPO_4$ deposits (6), and on different studies of their thermal stabilities (14). We have obtained by vector gas chromatography analysis the decomposition temperature of TBP ($\approx$400°C), and by thermogravimetric analysis, that of GaAA ($\approx$200°C) (14).

The alcoholic solution is contained in a glass vessel, the bottom of which is fitted with a piezoelectric transducer. The piezoelectric ceramic is excited at 770–780 kHz (i.e., close to its resonance frequency) and a geyser is formed at the liquid surface. The combined effects of cavitation within the liquid and waves at its surface produce an aerosol carried by a gas of controlled flow toward the pyrolysis region enclosed in a glass chamber (9). In our case, we used nitrogen with a flow rate of 180–300 liters/h. The direction of the gas flow is perpendicular to the horizontal substrate heated by a refractory furnace ($T_{max} = 500$°C). The gas flow selected and the heating plate design ensure that the deposition is a CVD process. The solvent is entirely vaporized close to the substrate. Substrates used are Si(100) and (111) and GaAs(100). Prior to deposition, they are cleaned with an aqueous solution of nitric and fluorhydric acids.

2. *Chemical Analysis by Energy-Dispersive Spectroscopy*

Depending on the coating temperature and the concentration of the starting solution, thin layers with different gallium, phosphorus, and oxygen proportions were obtained. A Kevex Sigma energy-dispersive X-ray spectrometer was used to check their chemical composition. The beam voltage and the beam current were respectively 5 kV and 1.24 nA. Under these conditions (beam penetration was 0.38 mm), the substrate was not involved since the thickness of the layers lies between 0.5 and 1 mm (see Section II.4). The standard used was pure $GaPO_4$ crystal. Gallium, phosphorus, and oxygen chemical compositions were found with a relative error of $\pm$ 0.5% for each atomic percentage. The composition of each sample is represented by the value of the concentration ratio:

(i) Ga : P, where Ga and P atomic concentrations are obtained from the X-ray analysis.

(ii) $O_{th} : O_{exp}$, where O_{th} is the amount of oxygen calculated by assuming that the Ga and P are present in the form of the oxides Ga_2O_3 and P_2O_5. Therefore, $O_{th} = 5:2$ (P) + 3 : 2 (Ga) and O_{exp} is obtained directly from the probe measurements (not by difference).

TABLE 1

Gallium Phosphate Thin Films (Si Substrate): Composition and Oxygen Excess in Connection with Coating Temperature and Initial Composition for the Precursor Ratio R = [GaAA]/[TBP] = 1/2

T (°C)	Ga : P	$O_{th} : O_{exp}$
384	0.68	1.00
375	2.06	0.88
372	2.87	0.92
364	3.14	0.95
358	3.31	0.92
347	3.79	0.79

Tables 1 and 2 show respectively the results obtained for deposits on Si and GaAs substrates. We have chosen to present the results obtained for the ratio R = [GaAA]/[TBP] = 1/2, where [GaAA] and [TBP] are precursor concentrations in alcoholic solution. First, we note that the composition Ga:P = 1; $O_{th} : O_{exp} = 1$, corresponding to the stoichiometric $GaPO_4$ phase, is never reached. Moreover, we observe a strong chemical composition evolution over the temperature range studied (345–385°C): the gallium content decreases as the substrate temperature increases. To explain this phenomenon, we hypothesize a competition between two reactions. The first would correspond to a reaction between the two precursors, tributyl phosphate and gallium acetylacetonate, resulting in formation of the $(O–Ga–O–P)_n$ linkage, and the second would be due to the cracking of the GaAA precursor alone at low temperature, resulting mainly in the formation of $(O–Ga–O–Ga)_n$ chains characteristic of the gallium oxide (Ga_2O_3). Indeed, the study of the thermal stability of the precursors has shown that the temperature decomposition of GaAA is near 200°C, and that of TBP, close to 400°C (14). This difference may

TABLE 2

Gallium Phosphate Thin Films (GaAs Substrate): Composition and Oxygen Excess in Connection with Coating Temperature and Initial Composition for the Precursor Ratio R = [GaAA]/[TBP] = 1/2

T (°C)	Ga : P	$O_{th} : O_{exp}$
384	0.70	1.00
378	2.41	0.91
374	2.61	0.88
364	3.41	0.80
358	3.65	0.80

explain the large increase in the Ga:P ratio with decreasing temperature over the temperature range studied.

Furthermore, we try to explain the "jump" in stoichiometry registered between 375 and 385°C. In alcoholic solution, solvolysis of the ester, $(C_4H_9)_3PO_4$, occurs, with formation of hydrogen phosphate ions. We can observe their condensation in the temperature range 350–450°C with formation of polyphosphate as pyrophosphate ($P_2O_7^{4-}$) (15). So, under the operative conditions, if the condensation of the hydrogen phosphate starts near 370°C for the solution ($R = 1:2$), it is normal to observe an excess of phosphorus and a discontinuity of the Ga:P ratio.

Another characteristic of these thin films is oxygen excess (Tables 1, 2), which is more important for the Ga-rich layers. This is directly related to the presence of proton-based impureties (OH^- and H_3O^+ species for neutral balance) as evidenced by infrared spectroscopy (16), due to a lower deposition temperature (350–360°C for Ga-rich layers), in accordance with previous works on aluminum phosphate films obtained by the "pyrosol" process (17).

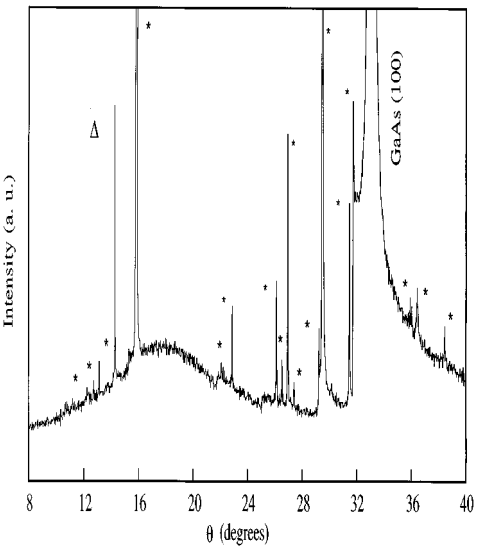

FIG. 2. X-ray diffraction pattern of a P-rich thin film deposited on GaAs substrate ($Ga:P \approx 0.70$; $O_{th}:O_{exp} \approx 1$). * β-Ga_2O_3; $^{\Delta}As_2O_5$.

3. X-ray Diffraction Analysis

X-ray diffraction experiments were made using a Seifert-JSO Debyeflex 1001 diffractometer (Cu$K\alpha$). Films obtained in the temperature range studied on silicon substrate were amorphous (Fig. 1). However, with respect to those obtained on GaAs substrate, X-ray diffraction patterns have shown crystallization of the β-Ga_2O_3 form (Fig. 2). This crystallization is favored by a thin native gallium oxide layer [grown during the time necessary to reach and to stabilize the coating temperature (14)] at the semiconductor surface, allowing the growth of epitaxial β-Ga_2O_3. On the other hand, the phosphorus-containing phase remained amorphous to X-rays.

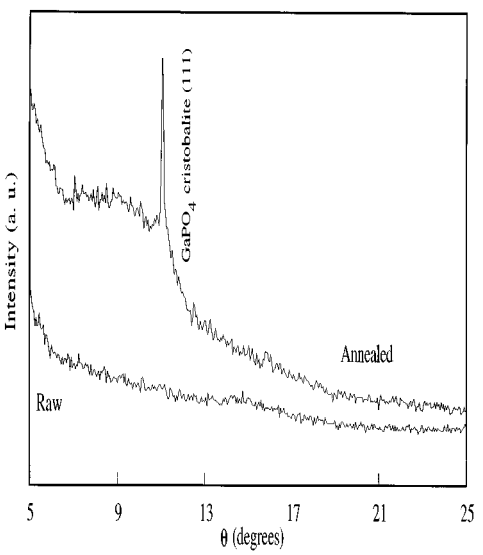

FIG. 1. X-ray diffraction pattern of a P-rich thin film deposited on Si substrate for air annealing of 48 h at 950°C (raw—$Ga:P = 0.76$, $O_{th}:O_{exp} = 0.99$).

To obtain the stoichiometric phase $GaPO_4$, which is a good dielectric material, we thermally treated the raw amorphous phosphate gallium layers deposited on Si substrate.

For P-rich thin films (Ga:P < 1), we registered the beginning of crystallization of the cristobalite $GaPO_4$ form after air annealing at 950°C for 48 h. The X-ray diffraction pattern (Fig. 1) indicates the presence of the (111) orientation, which is the main diffraction peak. On the other hand, Ga-rich deposits start to crystallize in the gallium oxide form β-Ga_2O_3 after 48 h of air annealing at 950°C (Fig. 3). Table 3 shows the annealing effect (48 h at 950°C) on the chemical composition of these deposits. We note, for all the compositions, an important reduction in oxygen excess ($O_{th}:O_{exp}$ tends toward 1) and a decrease in phosphorus concentration. The chemical composition evolution for $Ga:P > 1$ layers is likely due to P_2O_5 sublimation with a simultaneous water loss during the thermal treatment. On the other hand, for P-rich films, only P_2O_5 evaporation causes the Ga:P and $O_{th}:O_{exp}$ ratios to tend toward 1.

4. Deposition Rate and Morphology

A Leica S 260 scanning electron microscope was used to obtain thin-film microstructure and deposition rate. The beam voltage and the beam current were the same as in the chemical analysis by energy-dispersive spectroscopy (5 kV, 1.24 nA). Whatever the experimental conditions (vector gas, flow rate, and deposition temperature), the deposition rate

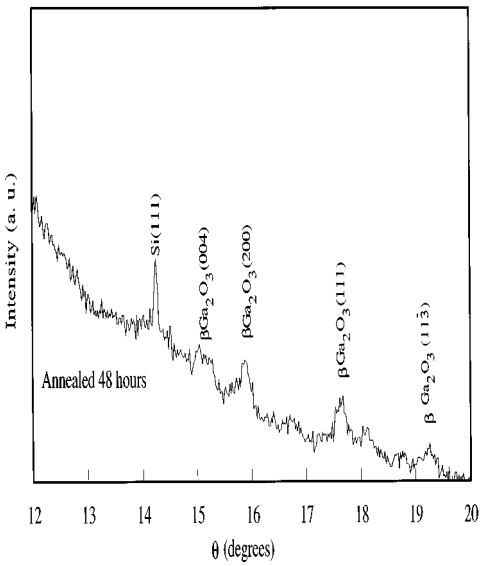

FIG. 3. X-ray diffraction pattern of a Ga-rich thin film deposited on Si substrate after air annealing for 48 h at 950°C (raw—Ga : P = 2.87, $O_{th} : O_{exp} = 0.92$).

of Ga-rich thin films (Ga : P > 1) is higher (≈2000 Å/h) than that of P-rich layers (300–400 Å/h). The thickness of the deposits lies between 0.5 and 1 μm for a deposition time close to 5 h. The microstructure of a raw thin film is presented in Fig. 4a. The film morphology depends on the Ga:P ratio. For Ga-rich deposits (Ga : P > 1), the surface appears smooth, without porosity. When the phosphorus content increases, the surface state is granular (Fig. 4a). The cross section of a P-rich deposit (Fig. 4b) shows a columnar structure. This type of growth is generally observed when the deposited material exhibits a high melting point [$T_{mp}(GaPO_4) = 1670°C$] (18–20). We have also observed this morphology for aluminum phosphate films [$T_{mp}(AlPO_4) = 1600°C$ (16)] obtained by the same process (6). The film morphology depends on the deposit conditions in relation to the pyrosol process, as explained by Viguié and Spitz (9). When deposits exhibit an excess of phosphorus, the process is one they called scheme D (9). In this scheme, at high temperature, the solvent is already completely vaporized far from the substrate and the chemical reaction takes place in the vapor phase. The molecules condense as microcrystallites, which form a powdery

TABLE 3
Comparison of the Chemical Compositions of Raw and Air-Annealed (48 h at 950°C) Thin Films Obtained on Si Substrate

Ga : P		$O_{th} : O_{exp}$	
Raw	Annealed	Raw	Annealed
0.76	1.00	0.99	0.99
0.89	0.95	0.94	1.00
2.06	2.57	0.88	1.00
2.84	3.53	0.92	1.00
3.21	4.04	0.87	1.00
3.67	5.20	0.80	0.99

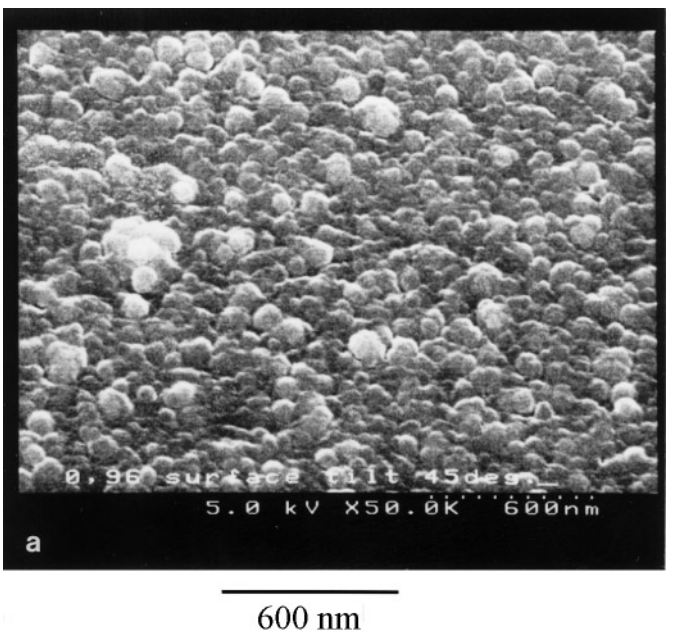

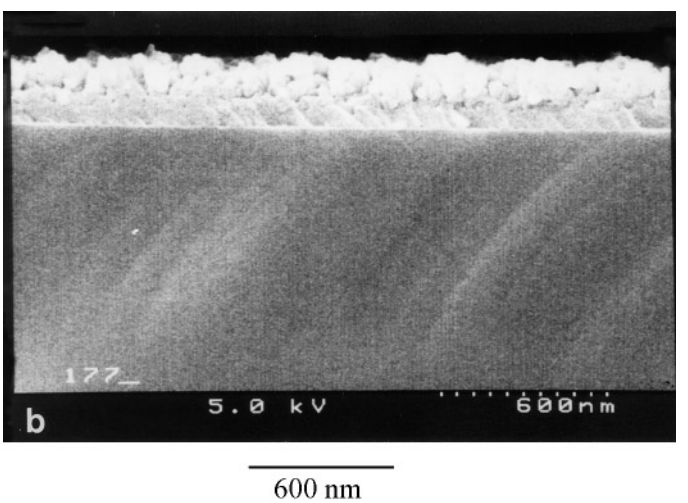

FIG. 4. Microstructures of raw gallium phosphate thin films deposited on Si. (a) Surface—Ga : P = 0.71, $O_{th} : O_{exp} = 0.93$. (b) Cross section—Ga : P = 0.71, $O_{th} : O_{exp} = 0.93$.

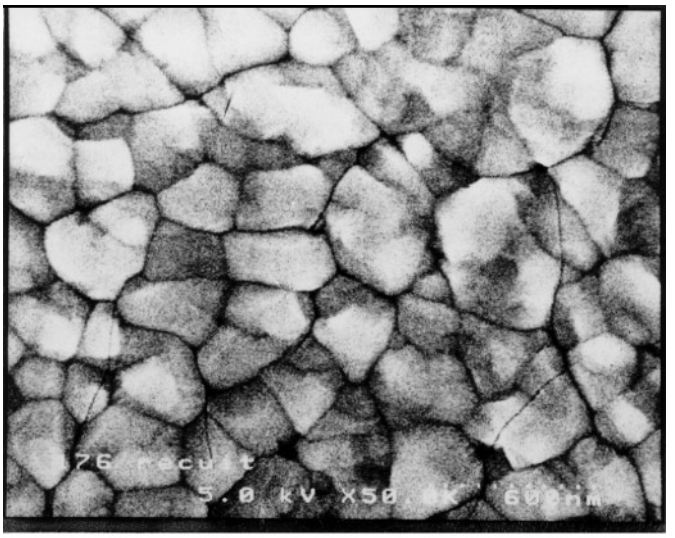

FIG. 5. Microstructure of air-annealed (48 h at 950°C) P-rich gallium phosphate thin film deposited on Si substrate.

precipitate on the substrate. In our case, P-rich deposits obtained by this scheme present a rough surface.

Figure 5 shows the microstructure of an air-annealed P-rich thin film. We can observe a densification of the structure. In this case, the diffusion of the elements involves the crystallization, then the densification of the structure, with formation of grains 300 nm in size. For air-annealed Ga-rich thin films, the microstructure (Fig. 6) appears crackled, with some white zones due to the presence of β-Ga_2O_3.

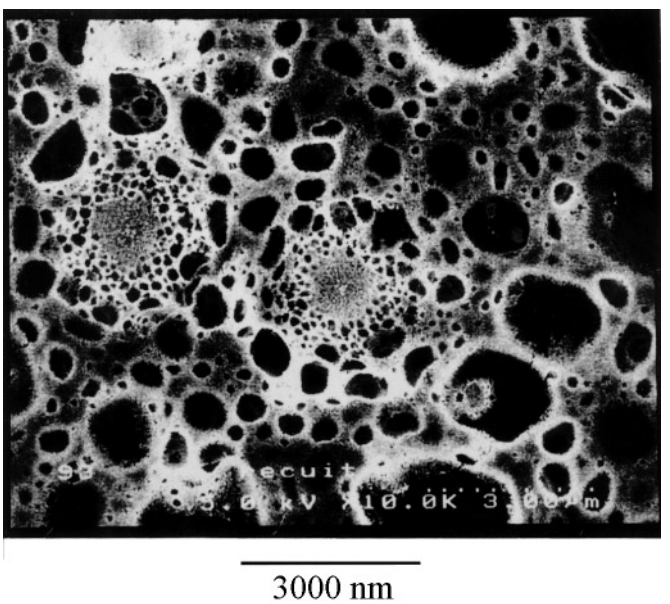

FIG. 6. Microstructure of air-annealed (48 h at 950°C) Ga-rich thin film deposited on Si substrate.

III. ELECTRICAL MEASUREMENTS

Electrical measurements were carried out on the MIS capacitor presented in Fig. 7. The semiconductors used were (100)-oriented p-type Si (B doped, $\rho = 2.5 \times 10^{-4}\ \Omega$ m) and n-type GaAs wafers (Si doped, $\rho = 2.6 \times 10^{-5}\ \Omega$ m). Si- or GaAs-doped substrate was used as one of the two electrodes; the other was made from a thin slice of platinum metal deposited by sputtering on the gallium phosphate layer. This MIS capacitor is inserted in a glass tube and kept under vacuum (10^{-3} Torr) throughout the measurement process. The capacitance and conductance of this system have been measured by using an impedance analyzer (Hewlett–Packard 4192A) over the frequency range 10^2 to 5×10^6 Hz and the temperature range 250 to 350 K. To reduce the phenomenon of electrode polarization of the MIS capacitor, electrical measurements were performed using alternating current (21, 22). Only raw deposits were studied, since for the annealed ones, the microstructure being crackled, electrical measurements were not possible.

1. *Results Obtained on the Pt/Gallium Phosphate Layer/Si System*

Component of the conductivity σ_{DC} under direct current. The direct conductivity σ_{DC} can be expressed as a function of temperature,

$$\sigma_{DC} = \sigma_0 \exp\left(\frac{-E_a}{kT}\right), \qquad [1]$$

where E_a represents the required energy for charge barrier hopping between localized sites, characteristic of the conduction mechanism at room temperature and corresponding to the material conductivity under direct current (limit value of σ_{DC} for angular frequency $\omega \to 0$). We have plotted, in Fig. 8, $\log(\sigma_{DC}) = f(1000/T)$ for raw samples of different

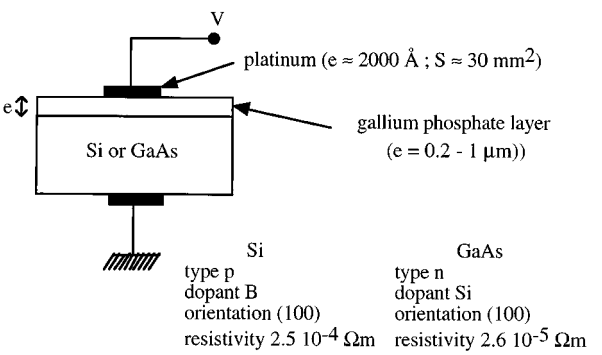

FIG. 7. Cross section of the MIS capacitor and characteristics of Si and GaAs substrates.

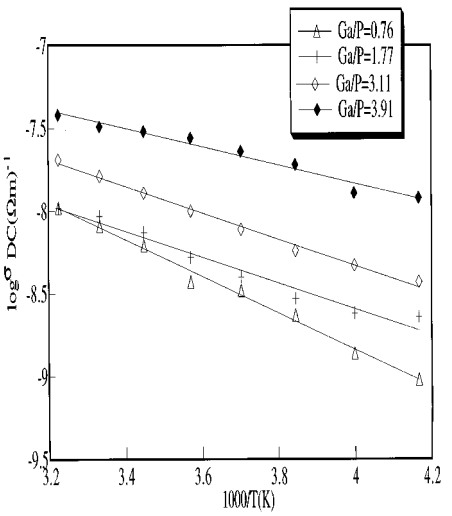

FIG. 8. Variation of $\log(\sigma_{DC})$ as a function of $1/T$ for different raw deposits of various compositions.

compositions deposited on Si substrate. $\mathrm{Log}\,(\sigma_{DC})$ varies linearly as a function of $1/T$ and increases with Ga and O content. σ_{DC} and E_a values obtained at room temperature for several compositions (Table 4) belong in the range where σ_{DC} can be expressed by Eq. [1]. These results, which are in agreement with those obtained for $AlPO_4$ thin films under direct (σ_{DC}) and alternative current (σ_{AC}) experiments (7), show that the residual conduction phenomenon can be explained by the correlated barrier hopping model developed by Elliott (23), which involves the lone electron pair of nonbridging oxygen atoms. Indeed, the presence of nonbridging oxygen atoms in these raw gallium phosphate layers has been pointed out with oxygen 1*s* core-level X-ray photoelectron spectroscopy (24). This explains why the conductivity is higher in the amorphous state than in the crystalline state.

Permittivity (ε'_r) *and dielectric loss* (ε''_r). Permittivity (ε'_r) was calculated from capacitance (C) measurements using the expression:

$$C = \frac{\varepsilon_0 \varepsilon'_r S}{e}, \qquad [2]$$

TABLE 4

Electrical Experimental Results Obtained under Direct Current (σ_{DC}, E_a) at 298 K versus Chemical Composition of Gallium Phosphate Thin Films Deposited on Si Substrate

Ga : P	$O_{th} : O_{exp}$	E_a (eV)	σ_{DC} $(\Omega\ m)^{-1}$ at $T = 298$ K
0.76	0.99	0.22	8.1×10^{-9}
1.77	0.89	0.16	9.3×10^{-8}
3.11	0.83	0.15	1.6×10^{-8}
3.91	0.83	0.11	3.2×10^{-8}

where ε_0 is the vacuum permittivity (8.85×10^{-12} F m^{-1}); S, the area of the capacitor (m^2); and e, the thickness of the capacitor (m) (Fig. 7). Dielectric loss (ε''_r) was calculated from conductance (G) measurements using the relation

$$\varepsilon''_r = \frac{G\varepsilon'_r}{\omega C}, \qquad [3]$$

where ω is the angular frequency. The temperature and frequency dependence of the dielectric constant (ε'_r) and dielectric loss (ε''_r) are respectively presented in Figs. 9a, 9b and 10a, 10b, for two different thin-film compositions obtained on Si substrate:

$\mathrm{Ga:P} = 2.59 \quad O_{th} : O_{exp} = 0.90 \quad$ Figs. 9a, 9b

$\mathrm{Ga:P} = 0.67 \quad O_{th} : O_{exp} = 0.99 \quad$ Figs. 10a, 10b

ε'_r and ε''_r behave in the same way. Permittivity and dielectric loss are nearly constant below room temperature, whereas an increase is observed above room temperature and the increase with temperature is frequency dependent: the lower the frequency, the higher the variation of ε'_r and ε''_r (Figs. 9, 10). This evolution is similar to that observed for $GaPO_4$ crystals (5). In the frequency range studied (1 kHz–1 MHz), the space charge polarization is the major contributor to the polarization mechanism. A direct consequence of the influence of charge polarization is that the dielectric constant and the dielectric loss decrease when frequency increases. This phenomenon is, as expected, accentuated at high temperature. Furthermore, the space charge polarization increases with oxygen concentration in the deposit ($O_{th} : O_{exp} = 0.90$, Figs. 9a, 9b). We have also observed this phenomenon in $GaPO_4$ crystals: the increase in permittivity and dielectric loss above room temperature could be attributed to the presence of "OH" impurity (5). In our case, the raw deposit of composition $\mathrm{Ga:P} = 2.59$ ($O_{th} : O_{exp} = 0.90$) produces dangling bonds Ga–O (21) and proton-based impurities (16). For P-rich thin films ($\mathrm{Ga:P} = 0.67$, $O_{th} : O_{exp} = 0.99$; Figs. 10a, 10b), the dispersion of ε'_r and ε''_r is less pronounced in relation to the decrease in oxygen excess.

2. *Results Obtained on the Pt/Gallium Phosphate Layer/GaAs System*

Films obtained on GaAs under the same conditions as on Si present the same chemical composition evolution versus substrate temperature (Tables 1 and 2). Figure 11 shows dielectric constant dependence on frequency for three different chemical compositions obtained on GaAs substrate. Electrical measurements realized under the same conditions as on Si show better dielectric properties [diminution in ε'_r ($3 < \varepsilon'_r < 7$) and ε''_r ($0 < \varepsilon''_r < 1$) dispersion], in agreement

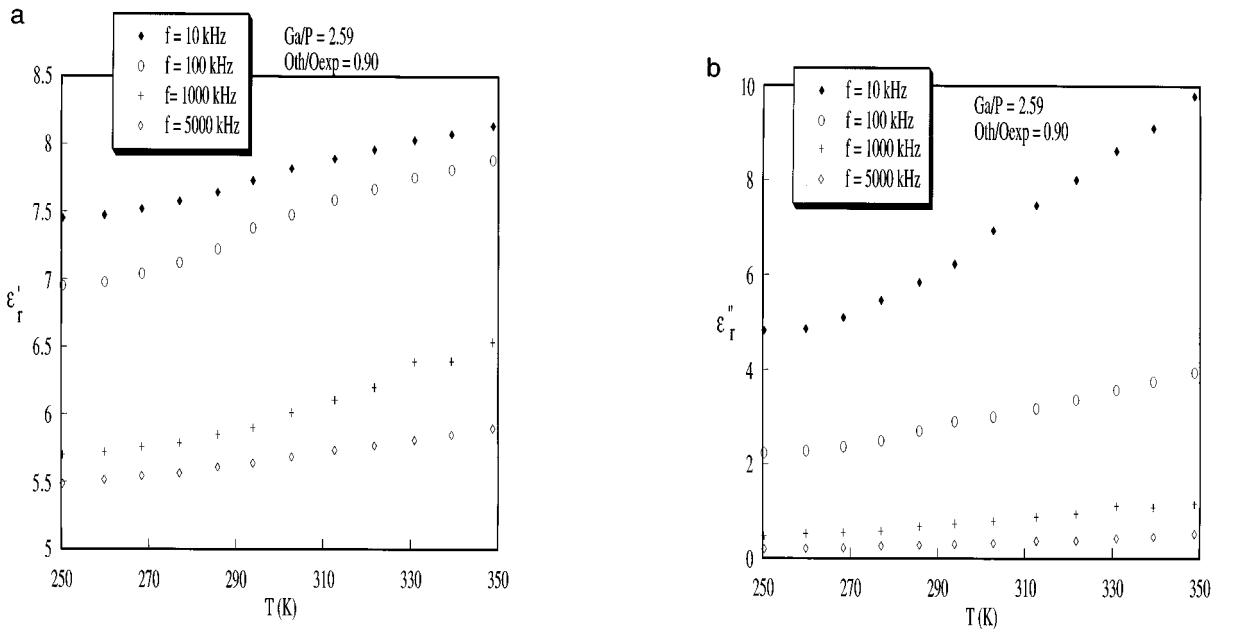

FIG. 9. Temperature and frequency dependence of dielectric constant ε_r' (a) and dielectric loss ε_r'' (b) of the gallium phosphate deposit (Ga : P = 2.59, $O_{th} : O_{exp} = 0.90$).

with the crystallization of the β-Ga_2O_3 form, for the raw deposits, which is a good dielectric material.

IV. CONCLUSION

This paper describes the characteristics of gallium phosphate thin films deposited by spray pyrolysis on Si and GaAs oriented substrates and their dielectric properties. Deposits obtained for concentrations of 0.025 *M* gallium acetylacetonate [$Ga(C_5H_7O_2)_3$] and 0.050 *M* tributyl phosphate [$(C_4H_9)PO_4$] were homogeneous, dense, and stable in the temperature range 250–400°C. They present a large composition range versus this temperature range. Whatever the deposition temperature, the raw thin layers

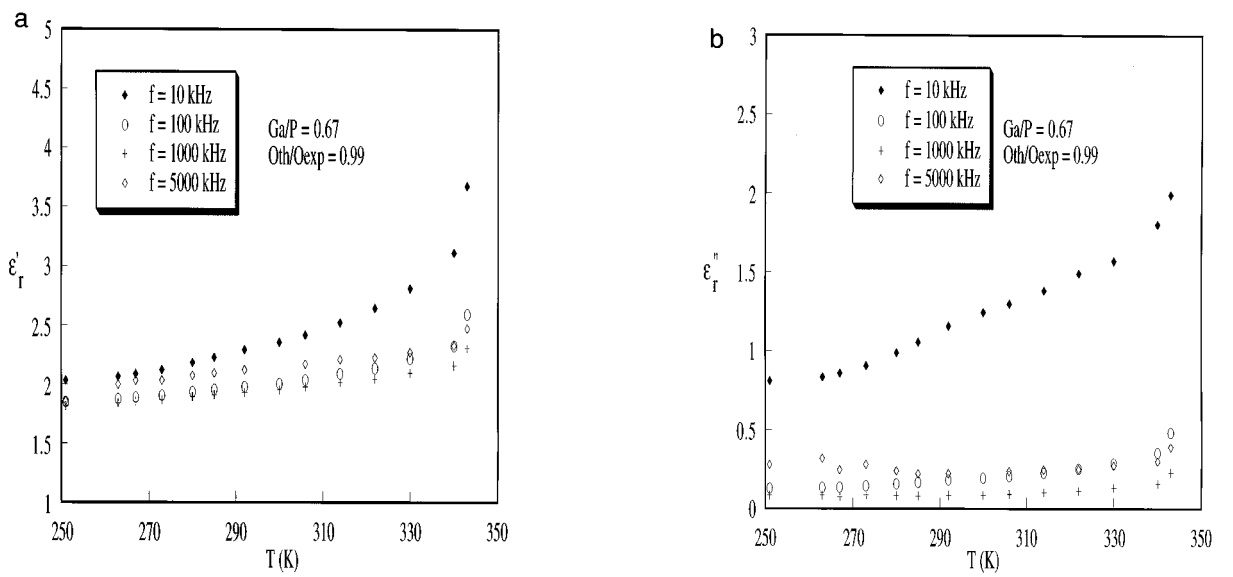

FIG. 10. Temperature and frequency dependence of dielectric constant ε_r' (a) and dielectric loss ε_r'' (b) of the gallium phosphate deposit (Ga : P = 0.67, $O_{th} : Oexp = 0.99$).

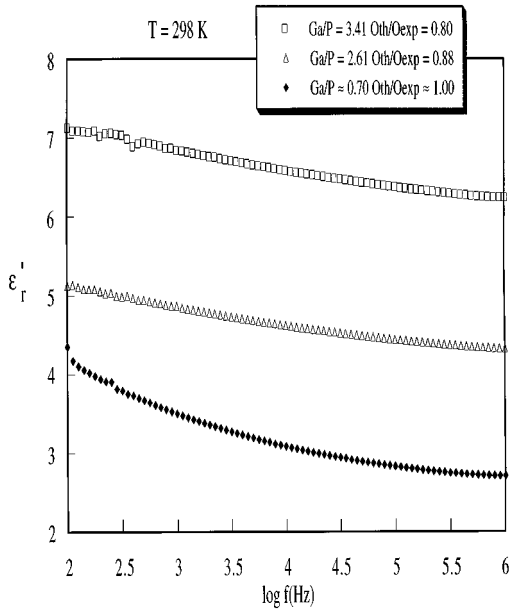

FIG. 11. Variation of permittivity (ε'_r) as a function of $\log f$ (Hz) at room temperature for deposits of various composition, obtained on GaAs substrate.

on Si are amorphous, whereas those obtained on GaAs are crystallized with the β-Ga_2O_3 form. On the other hand, phosphorus-containing phases remain amorphous. By annealing, the layers deposited on Si crystallize in the $GaPO_4$ cristobalite form for P-rich deposits and in the β-Ga_2O_3 form for Ga-rich deposits.

The electrical properties of these thin films are directly related to the oxygen excess due to the formation of nonbridging oxygen atoms and proton-based impurities. The first results obtained on GaAs substrate show that raw thin films crystallized in the β-Ga_2O_3 form exhibit better dielectric properties. Gallium oxide has proved to be a useful material for many applications, including metal–insulator structures on GaAs (25). Ga_2O_3 was obtained in different ways (26), but never by the "pyrosol" process, so, in a further work, we would like to synthesize gallium oxide thin films on GaAs substrate by this method and determine their dielectric characteristics.

REFERENCES

1. P. Viktorovitch, *Rev. Phys. Appl.* **25,** 895 (1990).
2. E. Philippot, A. Ibanez, A. Goiffon, M. Cochez, A. Zarka, B. Capelle, J. C. Schwartzel, and J. Détaint, *J. Cryst. Growth* **130,** 195 (1993).
3. E. Philippot, A. Ibanez, A. Goiffon, B. Capelle, A. Zarka, J. C. Schwartzel, and J. Détaint, *in* "Proceedings, 6th European Frequency and Time Forum," ESA SP 340. ESTEC, Noordwijk, 1992.
4. M. C. Record, A. Goiffon, J. C. Guintini, and E. Philippot, *J. Mater. Sci. Lett.* **9,** 895 (1990).
5. J. Foulon, J. C. Guintini, and E. Philippot, *Eur. J. Solid State Inorg. Chem.* **31,** 245 (1994).
6. S. Daviero, C. Avinens, A. Ibanez, J. C. Guintini, and E. Philippot, *J. Phys. III* **3,** 745 (1993).
7. S. Daviero, C. Avinens, A. Ibanez, J. C. Guintini, and E. Philippot, *J. Non-Cryst. Solids* **146,** 279 (1992).
8. S. Daviero, A. Ibanez, C. Avinens, A. M. Flank, and E. Philippot, *Thin Solid Films* **226,** 207 (1993).
9. J. C. Viguié and J. Spitz, J. *Electrochem. Soc.* **122,** 585 (1975).
10. W. Siefert, *Thin Solid Films* **121,** 275 (1984).
11. G. Blandenet, M. Court, and Y. Lagarde, *Thin Solid Films* **77,** 695 (1981).
12. G. T. Morgan and H. D. K. Drew, *J. Chem. Soc.* **119,** 1058 (1921).
13. O. B. Ajaggi, M. S. Akanni, and J. N. Lambi, *Thin Solid Films* **138,** 91 (1986).
14. F. Tourtin, Ph.D. thesis, Université Montpellier II, 1996.
15. J. R. Van Wazer, "Phosphorus and Its Compounds," p. 8. Interscience, New York, 1958.
16. F. Tourtin, P. Armand, A. Ibanez, A. Manteghetti, and E. Philippot, *Thin Solid Films* (1997).
17. S. Daviero, C. Avinens, A. Ibanez, C. Cambié, M. Maurin, and E. Philippot, *Vide Couches Minces* **250,** 23 (1990).
18. K. Kosten and H. Arnold, *Z. Kristallogr.* **152,** 119 (1980).
19. L. H. Cohen and W. Klement, *Phil. Mag.* **39,** 399 (1979).
20. A. Perloff, *J. Am. Ceram. Soc.* **39,** 83 (1956).
21. P. M. Sutton, *J. Am. Ceram. Soc.* **47,** 188 (1964).
22. D. L. Kinser and L. L. Hench, *J. Am. Ceram. Soc.* **52,** 638 (1969).
23. S. R. Elliott, *Adv. Phys.* **31,** 132 (1987).
24. F. Tourtin, P. Armand, A. Ibanez, G. Tourillon, and E. Philippot, *J. Mater. Chem.* (1997).
25. B. Hoeneisen, C. A. Mead, and M. A. Nicolet, *Solid State Electron.* **14,** 1059 (1971).
26. K. Ozasa, T. Ye, and Y. Aoyagi, *J. Vac. Sci. Technol. A* **1,** 120 (1994).